

Edge turbulence in RFX-mod virtual-shell discharges

P. Scarin ^{*}, M. Agostini, R. Cavazzana, F. Sattin, G. Serianni, N. Vianello

Consorzio RFX, Associazione Euratom-ENEA sulla Fusione, Corso Stati Uniti 4, Padova, Italy

Abstract

In the Reversed Field Pinch eXperiment RFX-mod a Gas Puffing Imaging Diagnostic (GPID) is used to investigate the dynamical structure of plasma edge turbulence. The GPID measures the radiation emitted from He gas puffed in H discharges and allows the investigation of edge plasma properties with high time and space resolution at high plasma current during the entire discharge. The characterization of edge turbulence has been carried out in terms of power spectrum, cross-correlation and toroidal velocity of structures. The scaling of such velocity with the density corresponds to different values of the dimensionless ratio ν_{ci}/ν_{ei} (ion cyclotron frequency/electron–ion collision frequency) ranging from below to above unity. The toroidal characteristic length of intermittent structures at different time scales has been determined by applying the conditional average technique on the structures identified by the continuous wavelet transform. These lengths are in the range 15–45 mm, while the number of structures increases with the electron density, the propagation velocity, opposite to the plasma current, decreases with the density and saturates at -20 km/s.

© 2007 Elsevier B.V. All rights reserved.

PACS: 52.35.Qz; 52.35.Mw; 52.35.Ra; 52.25.Gj

Keywords: RFP; RFX; $E \times B$ drift; Intermittency; Density limit

1. Introduction

The study of the mechanisms behind anomalous transport driven by plasma turbulence is a key issue in plasma magnetic confinement research.

Despite the rich magnetic activity which characterizes the configuration, the Reversed Field Pinch (RFP) has several similarities with Tokamaks and Stellarators. Among the most remarkable similarities is the observation that the edge particle transport is mostly driven by electrostatic fluctuations,

and electrostatic coherent structures have been observed to emerge from the turbulent background. These structures have been identified as intermittent bursts, i.e. ‘events’ higher-than-average occurring sporadically but more often than described by a Gaussian statistical distribution. Their contribution to anomalous particle transport has been estimated and can account for up to 50% of the total [1].

The RFP is a self-organized system where the plasma produces, through a dynamo mechanism, its own equilibrium characterized by a toroidal component of magnetic field reversed at edge with respect to the centre. A reversal parameter $F = B_{\phi}(\text{wall})/\langle B_{\phi} \rangle$ is commonly adopted to characterize the RFP equilibrium and is simply related to the

^{*} Corresponding author. Fax: +39 049 8700718.
E-mail address: paolo.scarin@igi.cnr.it (P. Scarin).

magnetic pitch at the wall. To sustain the dynamo some level of non-axisymmetric magnetic perturbations (modes) is required [2].

In order to better control magnetic boundary, some plasma control techniques have been devised. Recently in RFX-mod (major radius $R = 2$ m, minor radius $a = 0.46$ m) a virtual-shell (VS) configuration has been developed. It is obtained by a set of 4 (poloidally) \times 48 (toroidally) saddle coils, with independent power supplies. The control of the magnetic field at the boundary is achieved by a feedback system cancelling the local radial field at each saddle coil [3].

In this paper we consider discharges with plasma current in the range 500–800 kA, corresponding to ~ 20 MW ohmic heating, with average electron density up to $4 \times 10^{19} \text{ m}^{-3}$ and core electron temperature of about 400 eV.

To systematically study the dynamical structure of plasma edge turbulence under different plasma conditions the GPID system [4] has been used during the VS discharges, with pulse length up to 0.35 s. Helium gas is puffed in the hydrogen discharges and the emission of HeI (668 nm) line, I_{HeI} , is observed along 16 Lines of Sight (LoS), toroidally spaced by 5 mm, each 4 mm wide. As already reported elsewhere [5], it is difficult to unfold directly the density fluctuations from light emission fluctuations, but from Langmuir measurements in old RFX [6] of edge electron density and temperature, density fluctuations are about two times those of temperature. The He flux injected for the measurements is 10^{19} – 10^{20} atoms/s and it does not seem to influence the turbulence properties as evidenced by other edge diagnostic systems close to GPI in presence or absence of the He puff.

One of the parameters that affects the edge turbulence is the local distance $\lambda_w(\phi, \theta)$ of the last closed magnetic surface (defined by linear overlapping of

$m = 1$ and $m = 0$ poloidal modes) from the wall, which quantifies the local plasma deformation. Its value is negative when there is a gap between the well-confined plasma and the wall; its value is positive when magnetic field lines intercept the wall and the diagnosed volume is fully embedded into the main plasma. In this paper only measurements obtained with negative values of $\lambda_w(\phi, \theta)$ will be considered.

Plasma conditions can be characterized by the values of the reversal parameter F and of the ratio (I_p/N) between the plasma current and the linear electron density $N = \pi a^2 n$ (n is the volume-averaged electron density), the ratio I_p/N is equivalent to the inverse of the average electron density normalized to the Greenwald density n_G : $N/I_p \propto n/n_G$. Henceforth this latter parameter will be adopted, since also in RFPs a Greenwald density limit has been found [7].

2. Experimental findings

The following discussion of GPID experimental results is about the comparison between discharges with different densities, quantified in terms of the n/n_G parameter. A closer look at the signals of contiguous lines of sight indicates that randomly distributed high-intensity ‘bursts’ emerge from the background turbulence. In Fig. 1 I_{HeI} fluctuations are shown for two density regimes ($n/n_G \approx 0.35$ and 0.15, with reversal parameter $F = -0.1$) of the 16 LoS of the GPID, in a 100 μs time interval (time resolution of PMT is 0.5 μs). The amplitudes of the signals of 16 LoS have been each normalized to the own peak light emission in the considered time interval, to remove variations due to different PMT channel sensitivities. At the higher density more bursts emerge from background turbulence than at lower density. As long as the time evolution

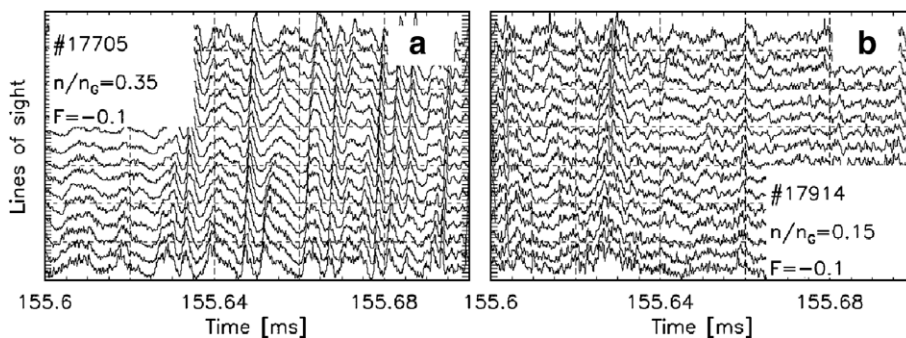


Fig. 1. Comparison of relative intensity bursts in two different density regimes: (a) high density; (b) low density.

is concerned, each LoS shows a similar pattern shifted in time, propagating toroidally from chord 1 to 16, in the direction opposite to plasma current, the same as the $E \times B$ drift flow. In order to quantify the propagation perpendicular to the main magnetic field, a cross-correlation analysis is performed for every pair of lines of sight, with an averaging interval of 0.2 ms. The maximum of the cross-correlation function presents a linear dependence on the chord position with the delay time, from which it is possible to calculate the toroidal velocity v_ϕ of fluctuations. In Fig. 2 the scaling of v_ϕ versus n/n_G is shown; each point is an average over 10 ms taken during the current flat-top. The experimental range of $0.1 \leq n/n_G \leq 0.7$ has been divided into ten intervals and the average values of v_ϕ in these ten ensembles have been considered. These values are shown with their statistical error bars. By comparing discharges with various values of n/n_G (after selecting $\lambda_w \leq -5$ mm) an increase of $|v_\phi|$ at lower density is evident, and the existence of a ‘critical’ density

at $n/n_G \approx 0.35$ is observed, above which a saturation of v_ϕ at a value of about -20 km/s is found. Although v_ϕ has not to be necessarily a fluid velocity, it has been found experimentally consistent, both in direction and absolute value, with an $E \times B$ drift [8,9] obtained from the radial gradient of plasma potential, measured with electrical probes at low plasma current.

The trend of v_ϕ versus n/n_G can be compared to the dimensionless parameter v_{ci}/v_{ei} evaluated at the edge. In a RFP the ion cyclotron frequency in the edge is $v_{ci} \approx 3 \cdot I_p/a$, while the electron–ion collision frequency $v_{ei} \approx 5 \times 10^{-11} \cdot n \cdot T_e^{-3/2}$ so the ratio becomes $v_{ci}/v_{ei} \approx a \cdot T_e^{3/2}/(500 \cdot n/n_G)$, (mks units, T_e in eV). An estimate of the edge electron temperature T_e in correspondence to critical density conditions ($n/n_G \approx 0.35$) gives a value of about 50 eV (where this value has been inferred from the scaling T_e versus I_p/N of the old RFX [10], measured with thermal He beam), so that the condition of ‘critical’ density becomes equivalent to $v_{ci}/v_{ei} \approx 1$. Thus the condition $n/n_G < 0.35$ would correspond to $v_{ci} > v_{ei}$ and the converse for $n/n_G > 0.35$. The threshold of $n/n_G \approx 0.35$ is an experimental result obtained in RFX-mod, that could represent a transition between different plasma regimes.

After the analysis of cross-correlation of the HeI emission signals it is interesting to consider the behaviour of their power spectra versus n/n_G to try to connect the different pieces information. In Fig. 3a the power spectra of one LoS are shown for two discharges with $n/n_G \approx 0.35$ and 0.15, where the power-law $f^{-\alpha}$ is respectively f^{-3} and f^{-2} in the frequency range 300–700 kHz. Fig. 3b gives the trend of the index α with n/n_G , for selected plasma shots ($\lambda_w \leq -5$ mm and $F = -0.13$ to -0.07), the selection in the reversal parameter is necessary to identify a scaling region. Each point corresponds

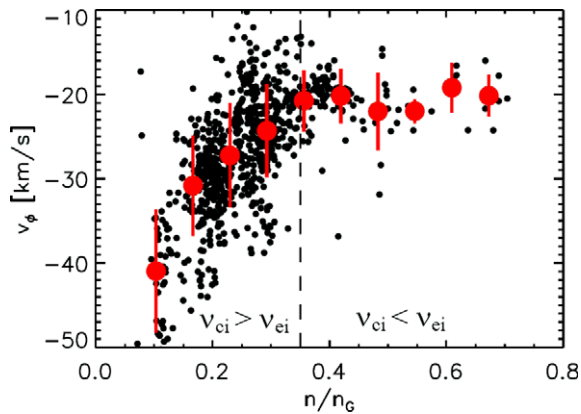


Fig. 2. Scaling of toroidal velocity v_ϕ of fluctuations with n/n_G parameter.

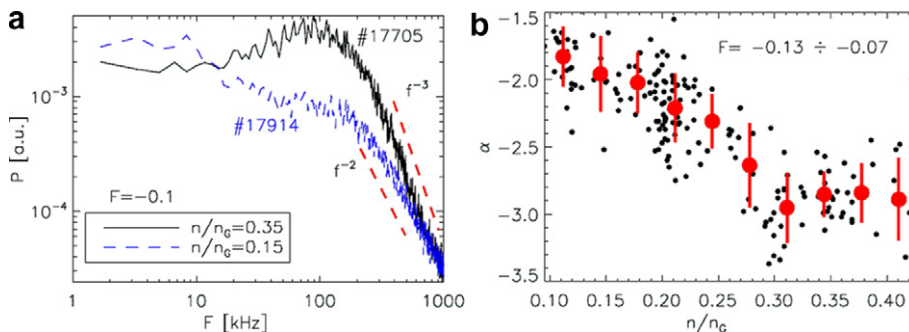


Fig. 3. Power spectra of HeI emission line: (a) comparison of a LoS for two different n/n_G values; (b) scaling of decay index α with n/n_G .

to a measurement of α in a time window of 10 ms. The useful experimental range for this scaling is $0.1 \leq n/n_G \leq 0.42$, which has been divided into ten intervals and the average value and statistical error of α for each interval has been considered (Fig. 3b). From the analysis of α versus n/n_G it is possible to recognize two regions: for $n/n_G < 0.3$ α decreases from -1.8 to about -3 and for $n/n_G > 0.3$ $\alpha \approx -3$.

A comparison of Figs. 2 and 3b suggests a trend of toroidal velocity of fluctuations v_ϕ versus the decay index α of the power spectrum.

3. Statistical analysis of emission fluctuations

Starting from the observations of the bursts in the I_{HeI} signals, as shown in Fig. 1 for the 16 radial LoS, a detailed analysis has been carried out to study the statistical properties of fluctuations at different time scales $\tau = 1/f$. By applying to these signals the Continuous Wavelet Transform (CWT), a set of wavelet coefficients $C_\tau(t)$ is obtained for each time series; $C_\tau(t)$ represents the time behaviour of characteristic fluctuations at each time scale τ [11]. The statistical properties of bursts are recognised from the PDFs [12] of the normalized wavelet coefficient fluctuations $\delta C_\tau / \sigma_\tau$ (σ_τ is the rms of $C_\tau(t)$). To quantify the weight of the tails with respect to the core of distribution, the scaling of flatness with τ has been considered: the flatness is defined as the ratio of the fourth-order moment of the distribution normalized to the square of the second-order moment; for a Gaussian distribution the flatness is equal to three. In the case of self-similar processes, the PDF of normalized fluctuation does not change its shape at different time scales. This reflects a constant flatness at all scales, whereas if the PDF of normalized fluctuations varies with the scales with an increasing of the tails of distribution at smaller scales the process is not self-similar and exhibits an intermittent character, implying an increase of flatness at smaller time scales. This analysis has been applied to compare discharges in different density regimes and with the same reversal parameter $F \approx -0.1$. In Fig. 4 the scaling of the flatness with the time scale τ for two values of n/n_G is shown: for a higher density discharge ($n/n_G \approx 0.35$) a non-self-similar behaviour is detected for time scales $1 \mu\text{s} < \tau < 10 \mu\text{s}$ (intermittency), instead for low density regimes ($n/n_G \approx 0.15$) non-Gaussian behaviour has been recorded in the same interval of time scales. For the analysis of PDFs, the flatness for all 16 LoS is evaluated in a time window of 20 ms

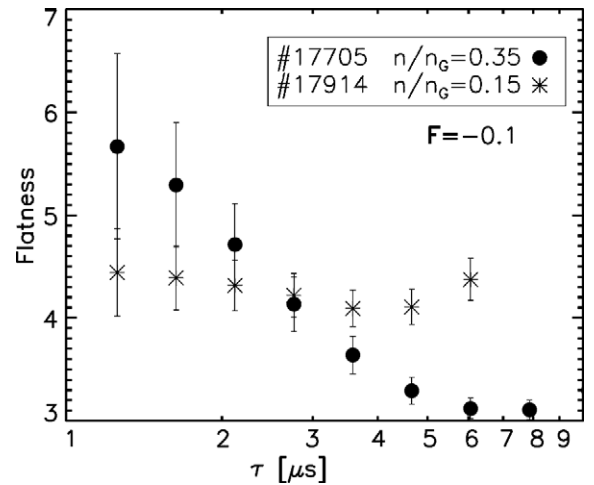


Fig. 4. Scaling of PDF flatness at different time scales τ for two density regimes.

and then the average in the 16 LoS ensemble is computed for each time scale. In Fig. 4, the result of the average is shown with statistical error bars.

Given the high spatial resolution of the optical diagnostic, it is possible to study the spatial features of intermittent bursts. Such analysis is carried out on the basis of conditional average technique, to outline the typical pattern of the bursts. For each LoS signal we consider the normalized fluctuations at their rms values. The reference signal is the intensity measured by the central chord of the fan and the 'prescribed condition' is the presence of a burst in the emission signal. A CWT has been applied to the reference signal to allow the detection of events on different time scales. An unambiguous characterization of burst presence at each time scale τ can be given by LIM (Local Intermittency Measure) technique [13]. From the simultaneous measurements of the intensity of the same burst on the 16 LoS it is possible to reconstruct the toroidal pattern of a single structure for different time scales. An estimate of the toroidal width of structures is obtained by averaging all the events at each time scale in a time portion Δt and superimposing a best fit of the form $\exp[-(x/\sigma)^2]$ over the obtained pattern. Fig. 5a displays the scaling of the toroidal width 2σ versus the fluctuation time scale for two different density regimes (n/n_G) in a time portion $\Delta t = 20$ ms: a non-linear increase from 15 mm to 45 mm in the range $1 \mu\text{s} < \tau < 10 \mu\text{s}$ is observed, whereas no clear difference appears for different density regimes. The number of structures detected at different time scales can be counted and after a normalization to

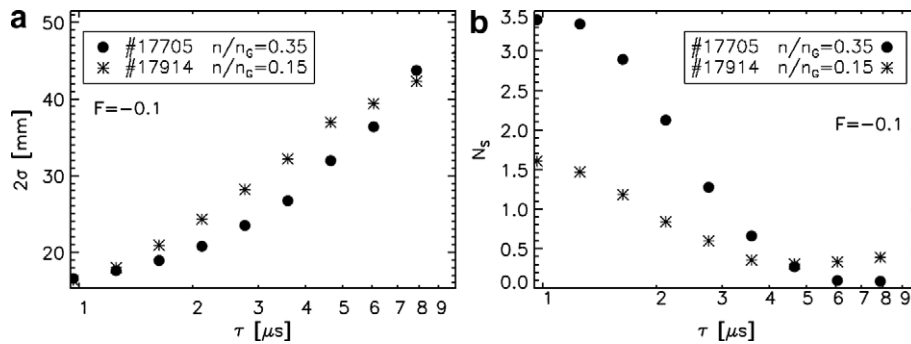


Fig. 5. Comparison of electrostatic structures for two n/n_G values: (a) scaling of the width 2σ versus τ ; (b) scaling of the number of structures N_S versus τ .

the measurement time portion Δt and to the toroidal propagation velocity v_ϕ , the number of structures N_S per unit length is obtained. In Fig. 5b the scaling of this number N_S versus time scale τ for two density regimes (n/n_G) is shown. There is an increase of N_S at small time scales ($\tau < 5 \mu\text{s}$) and the increase is particularly emphasized at the higher density regimes.

4. Summary

With the GPID a first experimental comparison of edge turbulence structures in RFX-mod has been carried out at different density regimes. A more detailed discussion about the meaning of these results and the description of the edge turbulence in RFX-mod with statistical analysis has been reported in [14]. Here the scaling of the toroidal velocity v_ϕ of emission fluctuations with the density has been shown to display a saturation value $v_\phi \approx -20 \text{ km/s}$ for high densities ($n/n_G \geq 0.35$), while for lower density an increase of $|v_\phi|$ can be noticed. This velocity v_ϕ is interpreted as a flow velocity and the scaling has been compared to the dimensionless parameter v_{ci}/v_{ei} . The power spectrum of I_{HeI} emission depends also on the parameter n/n_G . Analysis of fluctuations at different time scales yields probability distribution functions with non-

Gaussian tails at short time scales ($1 \mu\text{s} < \tau < 10 \mu\text{s}$). From the spatial resolution of electrostatic structures a toroidal width $15 \text{ mm} < 2\sigma < 45 \text{ mm}$ for time scales $1 \mu\text{s} < \tau < 10 \mu\text{s}$ has been measured; the number of structures increases at short τ values and more intermittent bursts are measured at higher density.

More systematic measurements need to be done to confirm the observed scaling, particularly at the highest ($n/n_G \geq 0.5$) and the lowest densities ($n/n_G \leq 0.15$).

References

- [1] M. Spolaore et al., Phys. Rev. Lett. 93 (2004) 215003.
- [2] S. Cappello, Phys. Contr. Fus. 46 (2004) B313.
- [3] R. Paccagnella et al., Phys. Rev. Lett. 97 (2006) 075001.
- [4] R. Cavazzana et al., Rev. Sci. Instrum. 75 (2004) 4152.
- [5] S.J. Zweben et al., Nucl. Fus. 44 (2004) 134.
- [6] E. Martines et al., Nucl. Fus. 39 (1999) 581.
- [7] M. Greenwald, Plasma Phys. Contr. Fus., 44 (2002) R27.
- [8] M. Spolaore et al., Phys. Plasma 9 (2002) 4110.
- [9] G. Serianni et al., in: 33rd EPS Plasma Physics Conf., Rome 2006, poster P5.096.
- [10] L. Carraro et al., Plasma Phys. Control. Fusion 42 (2000) 1.
- [11] M. Farge, Annu. Rev. Fluid. Mech. 24 (1992) 395.
- [12] V. Antoni et al., Europhys. Lett. 54 (2001) 51.
- [13] M. Onorato et al., Phys. Rev. E 61 (2000) 1447.
- [14] F. Sattin et al., Plasma Phys. Contr. Fus. 48 (2006) 1033.